ELSEVIER

Catalysis Today 73 (2002) 197–209

CATALYSIS TODAY

www.elsevier.com/locate/cattod

Catalytic activities of nickel-containing catalysts for ethylene dimerization and butene isomerization and their relationship to acidic properties

Jong Rack Sohn

Department of Industrial Chemistry, Engineering College, Kyungpook National University, Taegu 702-701, South Korea

Received 9 May 2001; accepted 28 September 2001

Abstract

Nickel oxide-silica catalysts were prepared by precipitation from an acidic solution of a nickel salt–sodium silicate mixture. Two types of nickel hydrosilicate, montmorillonite and antigorite are formed in the catalysts. Catalytic activities of nickel silicates for ethylene dimerization and butene isomerization run parallel when the catalysts are activated by evacuation at elevated temperatures, giving two maxima in activities. The variations in catalytic activities are closely correlated to the acidity of catalysts. The acid site responsible for the catalytic activity is protonic on montmorillonite, while non-protonic on antigorite, as evidenced by the effect of water content and the IR spectra of adsorbed pyridine. Catalytic activities of $NiO\text{-}TiO_2$ catalysts modified with H_2SO_4, H_3PO_4, H_3BO_3 and H_2SeO_4 for ethylene dimerization and butene isomerization were examined. The order of catalytic activities for both reactions was found to be $NiO\text{-}TiO2/SO_4^{2-} \gg NiO\text{-}TiO_2/PO_4^{3-} > NiO\text{-}TiO_2/BO_3^{3-} > NiO\text{-}TiO_2/SeO_4^{2-} > NiO\text{-}TiO_2$, showing clear dependence of catalytic activity upon acid strength. Catalytic activity of nickel sulfate supported on $\gamma\text{-}Al_2O_3$ ($NiSO_4/\gamma\text{-}Al_2O_3$) for ethylene dimerization is also closely correlated to the acidity of catalysts, showing that the active sites consist of a low-valent nickel (Ni^+) and an acid.

Keywords: Ethylene dimerization; Acidic properties; Active sites; Nickel-containing catalysts; Nickel silicates; $NiO\text{-}TiO_2$ modified with acids

1. Introduction

Nickel oxide on silica or metal oxide is an effective catalyst in olefin dimerization and isomerization as well as in the hydrocracking, oxidative coupling of methane and hydrogenation process following reduction of the nickel component [1–7]. One of the remarkable features of this catalyst system is its activity in the relation to a series of *n*-olefins. In contrast to usual acid-type catalysts, the nickel oxide on silica or silica-alumina shows a higher activity for a lower olefin dimerization, particularly for ethylene [3,4,8]. The catalyst is also active for the isomerization of *n*-butenes, the mechanism of which has been proved to be of a proton donor–acceptor type [9]. In the previous papers from this laboratory, it has been shown that $NiO\text{-}TiO_2$ and $NiO\text{-}ZrO_2$ modified with sulfate ion are very active for ethylene dimerization [10–12]. High catalytic activities in the modified catalysts in the reactions were attributed to the enhanced acidic properties of the modified catalysts. The enhanced acidic properties originate from the inductive effect of S=O bonds of the complex formed by the interaction of oxide with sulfate ion. A transition metal can also be supported on zeolite in the state of a cation or a finely dispersed metal. Several papers

E-mail address: jrsohn@knu.ac.kr (J.R. Sohn).

0920-5861/02/$ – see front matter
PII: S0920-5861(01)00513-2

have treated ethylene dimerization on transition metal cation-exchanged zeolites [13–15]. It was reported that Ni, Rh and Pd-exchanged zeolites were active for ethylene dimerization, while Cr-exchanged zeolite was active for ethylene polymerization.

It was previously reported that the dimerization activity is related to acidic property of the catalyst [2,16], by which the isomerization of butene proceeds. In this view, the role of acid site would be important in the mechanism of dimerization, although acid sites alone can not act as effective sites as those on $NiO\text{-}SiO_2$ for the dimerization of ethylene. In this paper, the correlations between dimerization and isomerization activities and acidic properties have been studied using several nickel-containing catalysts.

2. Experimental

2.1. Catalysts

Nickel oxide-silica was prepared by adding sodium hydroxide solution (0.1N) slowly into a mixed aqueous solution of sodium silicate, nickel sulfate or nitrate and sulfuric or nitric acid at 60 °C with stirring until the pH of mother liquid reached a certain value and then by allowing the precipitate to stand for 3 h at room temperature. The precipitate thus obtained was washed thoroughly with distilled water and was dried at 120 °C. The dried precipitate was again washed with successive portions of a 5% ammonium nitrate solution and then with hot distilled water to remove sodium ion remaining in the catalyst.

The modified $NiO\text{-}TiO_2$ catalysts were prepared as follows. The co-precipitate of $Ni(OH)_2\text{-}Ti(OH)_4$ was obtained by adding aqueous ammonia slowly into a mixed aqueous solution of nickel chloride, titanium tetrachloride and hydrochloric acid at room temperature while stirring until the pH of the mother liquid reached about 7. The precipitate thus obtained was washed thoroughly with distilled water until chloride ion was not detected and was dried at room temperature for 12 h. The dried precipitate was powdered below 100 mesh and then modification with acids was performed by pouring each 30 ml of 1N H_2SO_4, H_3PO_4, H_3BO_3 and H_2SeO_4 into 2 g of the powdered sample on a filter paper, followed by drying in air. The resultant solids were used as catalysts after decomposing at different evacuation temperatures for 1.5 h. The catalysts modified with H_2SO_4, H_3PO_4, H_3BO_3 and H_2SeO_4 are referred to as $NiO\text{-}TiO_2/SO_4^{2-}$, $NiO\text{-}TiO_2/PO_4^{3-}$, $NiO\text{-}TiO_2/BO_3^{3-}$, $NiO\text{-}TiO_2/SeO_4^{2-}$, respectively.

The catalysts containing various nickel sulfate content were prepared by impregnation of $\gamma\text{-}Al_2O_3$ powder (JRC-ALO-2, surface area $= 240\,m^2\,g^{-1}$) with aqueous solution of $NiSO_4{\cdot}6H_2O$ followed by calcining at 600 °C for 1.5 h in air. This series of catalysts are denoted by their wt.% of nickel sulfate. For example, $20\text{-}NiSO_4/\gamma\text{-}Al_2O_3$ indicates the catalysts containing 20 wt.% $NiSO_4$.

3. Procedure

The FTIR spectra were recorded at room temperature with a Mattson model GL 6030E spectrometer. Usually 2 mg of catalyst was mixed with 150 mg of KBr and pressed into a disk ($600\,kg\,cm^{-2}$). The FTIR spectra of some samples were obtained in a heatable gas cell at room temperature. The self-supporting catalysts wafers contained about $9\,mg\,cm^{-2}$. Prior to obtaining the spectra, the samples were heated under vacuum at 400–600 °C for 1 h. X-ray diffraction patterns of catalysts were taken by a Philips X'pert-APD diffractometer using a copper target and a nickel filter at 30 kV and 800 cps. X-ray photoelectron spectra (XPS) were obtained with a VG scientific model Escalab MK-11 spectrometer. AlKα and MgKα were used as the excitation source, usually at 12 kV, 20 mA. The analysis chamber was 10^{-9} Torr or better and spectra of samples, as pressed wafer, were analyzed.

The catalytic activity for ethylene dimerization was determined at 20 °C by a conventional static system following pressure change from an initial pressure of 280 Torr. Fresh catalyst sample was used for every run after evacuation at different temperature for 1 h. The isomerization of 1-butene was carried out at 20 °C in a closed circulating system. Reaction products were analyzed by gas chromatography with a VZ-7 column at room temperature. The specific surface area was determined by adsorption of N_2 at −196 °C.

Acidity of non-colored catalyst was determined by *n*-butylamine titration in benzene using dicinnamalacetone as the indicator, while chemisorption of ammonia was employed as a measure of acidity

of colored catalysts. The amount of chemisorption was obtained as an irreversible part of adsorption of ammonia [17].

4. Results and Discussion

4.1. Structure of $NiO\text{-}SiO_2$ catalysts

The precipitation from a mixed $NiSO_4$:Na_2SiO_3 (1:4) solution with sodium hydroxide was terminated at different pH values from 6 to 12.7. This series of catalysts is denoted by symbol A followed by the final pH value. Although the composition of starting material was the same, the NiO content increased with increase in pH, particularly at pH values above 6 and 10 as shown in Fig. 1, where the NiO content was determined by chemical analysis. The change at pH 6 is natural because the precipitation of $Ni(OH)_2$ takes place at this region [3], while the change above pH 10 is most likely caused by loss of silica into solution because of a high pH value. Fig. 1 also shows that the specific surface area decreases with increase in pH after a maximum at pH 6.7.

The structure of catalyst calcined at 550 °C was examined by IR spectroscopy. The IR spectra of catalysts A-6.7 to A-11 are given in Fig. 2. When they are compared with IR spectra of nickel oxide and silica as shown in Fig. 3, it is clear that new bands are formed at 420, 665 and 710 cm^{-1}, except for the catalyst A-6.7 and that the band at 800 cm^{-1} characteristic of silica decreases with increase in pH and is completely lost from A-11. The IR spectra of A-12 and A-12.7 were identical to that of A-11. Thus, the enrichment of NiO is evidently caused by dissolution of silica.

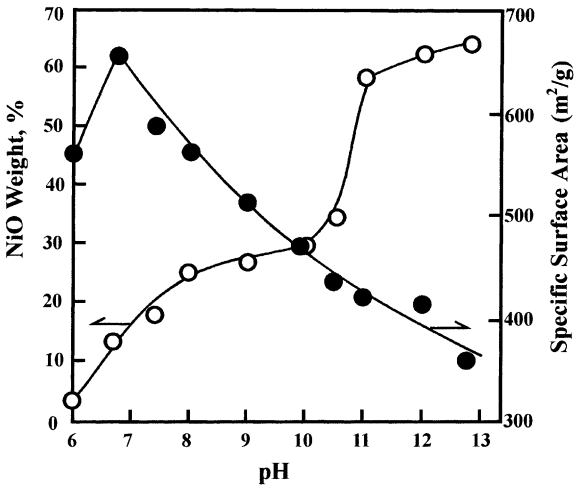

Fig. 1. Nickel oxide content and surface area of A-series catalysts as functions of pH in preparation.

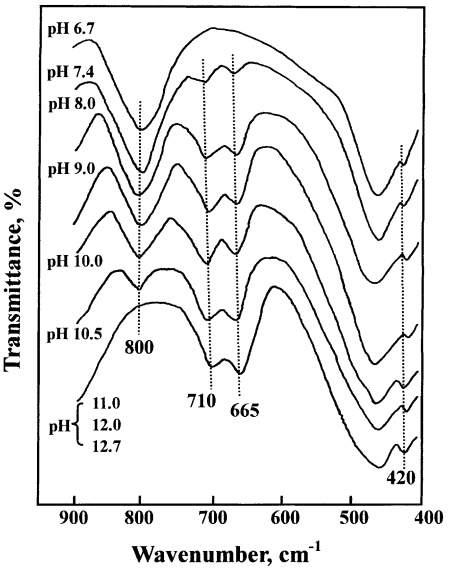

Fig. 2. IR spectra of A-series catalysts calcined at 550 °C.

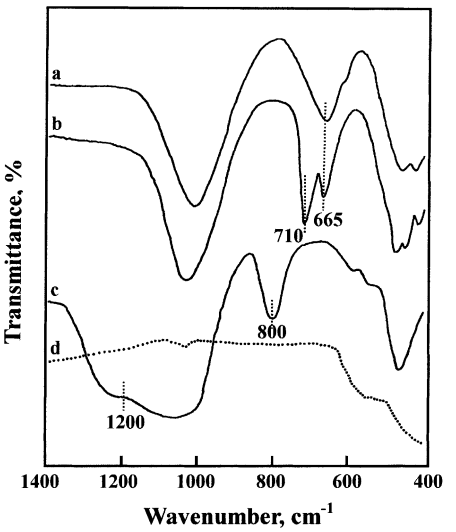

Fig. 3. IR spectra of: (a) sample II (nickel antigorite); (b) sample I (nickel montmorillonite); (c) silica gel; (d) nickel oxide.

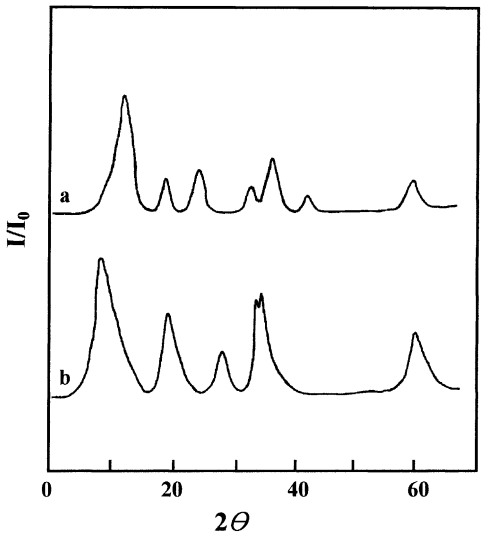

Fig. 4. X-ray diffraction patterns of nickel layer silicates synthesized by hydrothermal treatment: (a) nickel antigorite; (b) nickel montmorillonite.

Since, two types of nickel silicate of layer structure, nickel montmorillonite [$Ni_3(Si_2O_5)_2(OH)_2$] and nickel antigorite [$Ni_3Si_2O_5(OH)_4$], are known [3], two samples of nickel hydroxide precipitated on silica gel, which were different in NiO content (I (24%) and II (80%)), were subjected to hydrothermal treatment at 265–270 °C (50–54 atm) for 30 h. As shown in Fig. 4, the X-ray analyses showed that the nickel silicates formed in the samples I and II are montmorillonite and antigorite, respectively, as evidenced by *d* values of 9.4 and 3.1 Å (Mont.), and 7.4 and 3.6 Å (Ant.) [18]. However, for usual samples without hydrothermal treatment, the cubic phase of NiO (2θ values: 37.3, 43.3 and 62.9°) except for nickel silicates was observed in X-ray diffraction patterns, while the characteristic pattern of silica was not detected because silica was present as an amorphous phase. The IR spectra of the two samples are shown in Fig. 3. It is clear that the new bands found with catalysts A-7.4 to A-11 are ascribed to the silicates. Both 710 and 665 cm^{-1} bands have been assigned to Si–O stretching affected by Ni^{2+} for nickel talc and crysotile [19].

It is notable in Fig. 3 that the band intensity at 710 cm^{-1} is much stronger than that at 665 cm^{-1} with montmorillonite, while only the 665 cm^{-1} band is observed with antigorite. Thus, the two silicates can be distinguished by relative intensities of the two absorption bands. In view of this fact the spectra shown in Fig. 2 seem to show that the nickel silicate formed in the catalyst sample changes from montmorillonite to antigorite as the NiO content of catalyst or the final pH in precipitation increases. In fact, A-8 gave an X-ray diffraction pattern characteristic of montmorillonite, while A-11 gave a broad peak which can be ascribed to antigorite.

In view of the foregoing results, another series of catalysts were prepared starting from different composition of $Ni(NO_3)_2$–Na_2SiO_3–HNO_3 solution in which the concentration of HNO_3 was fixed at 1.5N. The precipitation by sodium hydroxide was terminated at a fixed pH of 7.5. This series of catalysts are denoted by symbol B followed by NiO content (wt.%) after calcination. In separate experiments, IR spectra of B-series of catalysts calcined at 550 °C were examined (not shown in the figure). It was seen that the relative intensity of the 710 cm^{-1} band to the 665 cm^{-1} band changes markedly between B-56 and B-66, indicating a change in the silicate species from montmorillonite to antigorite. Since NiO content in the antigorite is 65%, the changes at around this composition are quite reasonable.

Thus, it may be concluded that the nickel silicate species formed in the precipitate changes from montmorillonite to antigorite as the nickel oxide content increases and that the change can be monitored by IR spectra of calcined sample.

4.2. Ethylene dimerization activity of NiO-SiO_2 catalyst

In the Fig. 5, the ethylene dimerization activities per surface area of A-series of catalysts are plotted against the evacuation temperature at which the catalysts was pre-treated for 1 h. All of these catalysts exhibit two maxima of dimerization activity at 100 and 550–650 °C and a minimum at 200–350 °C as reported previously [16]. It is notable that the value at the second maximum is more extensively affected by the final pH in the catalyst preparation. Although the increase in final pH gives rise to the formation of antigorite, it is accompanied by an increase in nickel oxide content.

It is suggested by the results that there are two types of active sites which are closely related to the two nickel silicates. The montmorillonite-type

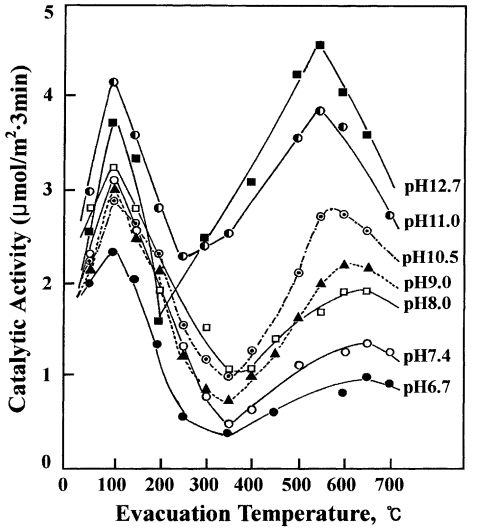

Fig. 5. Variations of catalytic activity of ethylene dimerization on A-series catalysts with evacuation temperature.

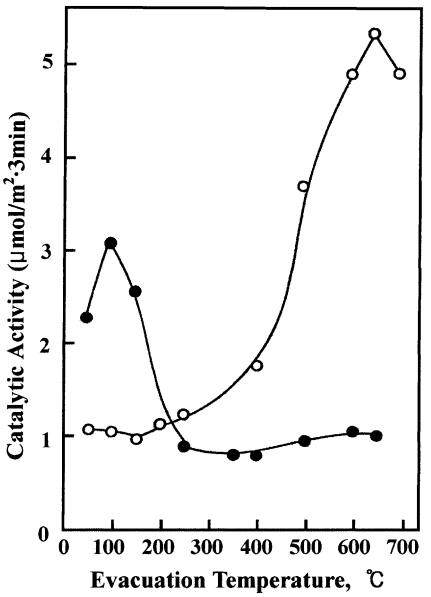

Fig. 6. Variations of ethylene dimerization activity with evacuation temperature: (●) B-4 catalyst; (○) B-85 catalyst.

(type M) sites are activated by evacuation at room temperature up to 100 °C, while the antigorite-type (type A) sites are activated above 250 °C up to about 600 °C. If this is the case, the twin peak activation curve as shown in Fig. 5 should be simplified by purifying the active sites. As shown in Fig. 6, both catalysts B-4 and B-85 also exhibit single but different maxima at 100 and 650 °C, respectively. It is reasonable that the low nickel oxide content in B-4 gives rise to little chance to form antigorite, resulting in exclusive formation of montmorillonite, while in B-85 antigorite is exclusively formed because of the high nickel oxide content.

It is thus very likely that there are two types of active sites and that the difference in their optimum activation temperatures is traced back to the difference in silicate structures. In the structure of antigorite, one silica layer of the type $Si_2O_5^{2-}$ is combined with an octahedral layer of the type $Ni_3^{2+}(OH)_6$, while in montmorillonite, one octahedral layer is sandwiched between two silica layers, in conformity with the formulas:

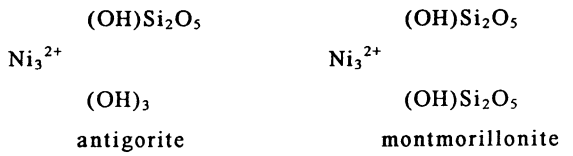

Thus, the OH groups bound to Ni^{2+} are located inside the silica layers of montmorillonite, while in antigorite, they are mostly exposed to the basal plane. Although, it is uncertain whether active sites are formed on basal planes or on edge planes, the above difference in the coordination states of the nickel ion should give rise to the observed difference in activation temperature.

4.3. Correlation between activities for ethylene dimerization and butene isomerization

It has been shown that the catalytic activity of $NiO\text{-}SiO_2$ for ethylene dimerization varies with temperature of pre-treatment (evacuation), giving two optimum temperatures, around 100 and 600 °C. The dimerization activity of A-10 changed with the evacuation temperature as shown in Fig. 7. In Section 4.2, the two activity peaks were ascribed to two different types of active sites, montmorillonite (100 °C) and antigorite (600 °C). The activity decrease by pre-treatment at high temperatures above 600 °C is reasonably explained by sintering or soild-phase rearrangement of the catalyst as demonstrated by irreversible decrease of specific surface area as well as the activity.

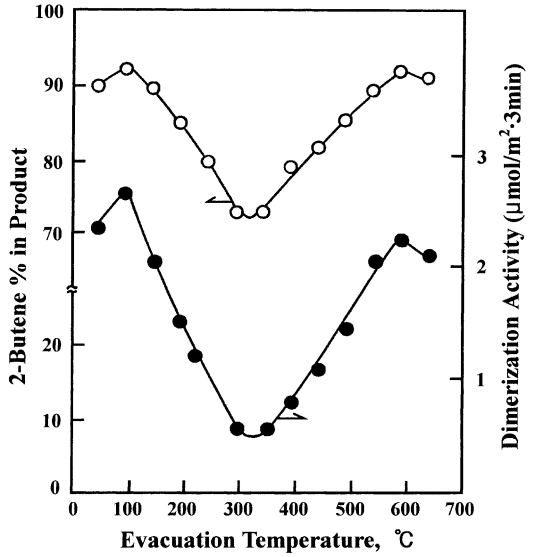

Fig. 7. Variations with evacuation temperature of catalytic activity and product composition in ethylene dimerization on catalyst A-10 at 20 °C.

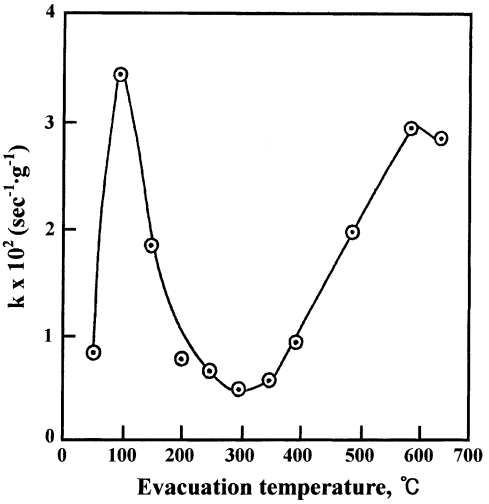

Fig. 8. Variation of 1-butene isomerization activity of catalyst A-10 with evacuation temperature.

It was found that the activity decrease is accompanied by a decrease in the extent of isomerization of *n*-butene produced by the dimerization. The compositions of *n*-butene obtained by dimerization runs on A-10 catalyst for 30 min are plotted against the evacuation temperatures in Fig. 7. It is obvious that the selectivity to 2-butene runs parallel with dimerization activity. Since the initial product of ethylene dimerization seems to be 1-butene [16], the above result suggests that the isomerization activity runs parallel with the dimerization activity. Thus, the isomerization of 1-butene was carried out at 20 °C on the catalyst A-10 in a circulating system. The time course of isomerization was in agreement with the first order rate law. Thus, the isomerization activity is represented by the first order rate constant. As shown in Fig. 8, it is confirmed that the isomerization activity also gives two maxima and one minimum at the same pre-treatment temperatures as those for the dimerization activity.

The above results are in conformity with the view that 1-butene is the initial product of ethylene dimerization. This view was further confirmed by the following experiments. In order to avoid the secondary isomerization of initial product, a cold trap cooled to −160 °C by isopentane bath was put in the circulating system and the catalyst bed height was minimized (about 10 mm). The partial pressure of ethylene was lowered to 4.5 Torr or lower. By taking these precautions, 1-butene was found to predominate (above 90 %) in the products of dimerization runs at 20 °C on B-10 catalyst evacuated at 100 °C.

4.4. Correlation between catalytic activity and acidity

Since, it was found in the present study that the isomerization activity also decreases by the evacuation at above 100 °C, the acidity responsible for the isomerization also should decrease. The acidities of catalyst A-6 thus determined are given as a function of evacuation temperature in Fig. 9 using dicinnamalacetone ($pK_a = -3.0$) as an indicator, where dimerization and isomerization activities are also given. It is clear that the catalytic activities decrease with decrease in acidity when the catalyst is evacuated at above 100 °C, confirming the above hypothesis. In this experiment the catalyst A-6 was chosen because of its lightness in color associated with low NiO content. The dimerization activity of A-6 is accordingly of the montmorillonite type, i.e. less active when evacuated at higher temperatures as shown in Fig. 9.

The antigorite-type catalyst, on the other hand, gives maximum activity when evacuated at 600 °C. Thus the acidity measurements were carried out with

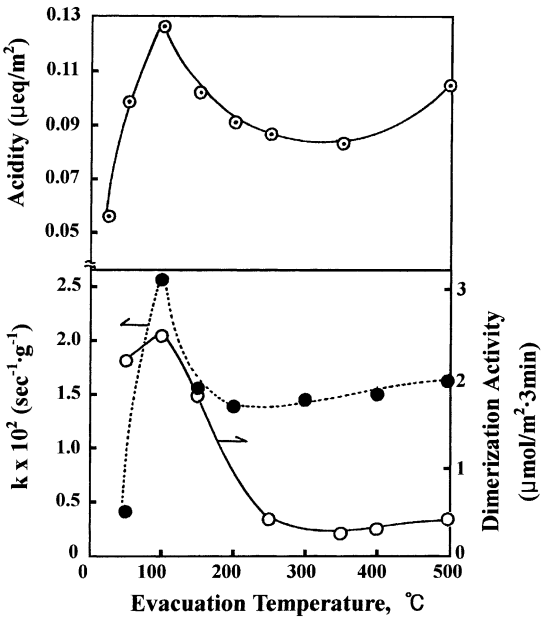

Fig. 9. Variations with evacuation temperature of acidity and catalytic activities for 1-butene isomerization and ethylene dimerization of A-6.

the B-series of catalysts evacuated at 600 °C employing the ammonia chemisorption method. The specific acidities per surface area are shown as a function of NiO content in Fig. 10, where the activities for dimerization and isomerization are also given. Both of the activities as well as the acidity increase with increase in NiO content up to 70 or 80% NiO, again disclosing parallelism between them. Since, those values are normalized by surface area, their variations with the NiO content demonstrate that the nature of active site changes from montmorillonite type to antigorite type with increase in the NiO content. In this way it is demonstrated that the catalytic activities of NiO-SiO_2 substantially run parallel to the acidity.

It has been established that protonic and non-protonic acid sites are distinguishable by IR absorption spectra of adsorbed pyridine [20]. Fig. 11 shows the IR spectra of pyridine adsorbed on catalyst A-7.4. Both the pyridinium ion band at 1543 cm^{-1} and the coordinated pyridine band at 1450 cm^{-1} are found with the catalyst evacuated at 100 °C, while only the latter is found with the catalyst evacuated at 400 °C. It is clear that the protonic acid sites are lost by the increase in evacuation temperature.

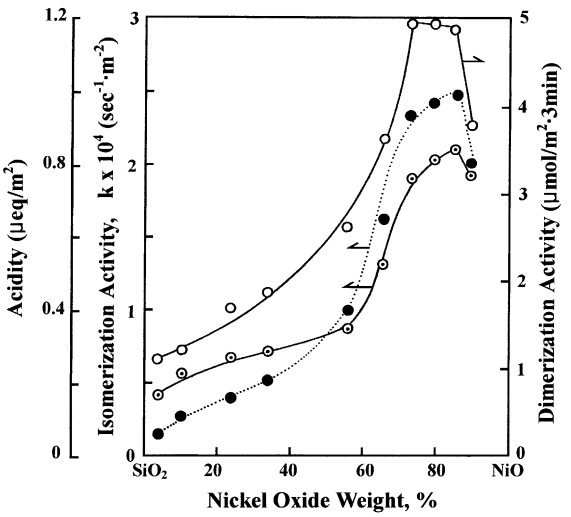

Fig. 10. Acidity and catalytic activities for 1-butene isomerization and ethylene dimerization as functions of NiO content of B-series catalysts: (○) ethylene dimerization activity; (●) 1-butene isomerization activity; (⊙) acidity.

4.5. Reactivation of deactivated catalyst

It has been shown that the activation of NiO-clay by evacuation at elevated temperatures is caused by dehydration from the surface because when the catalyst is exposed to water vapor after evacuation at a high

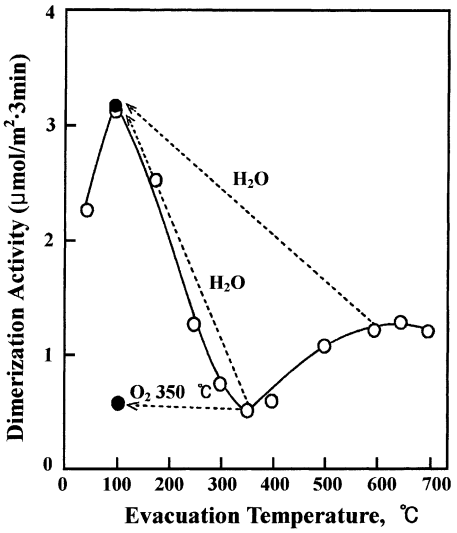

Fig. 11. Reactivation of deactivated catalyst (A-7.4) by water treatment.

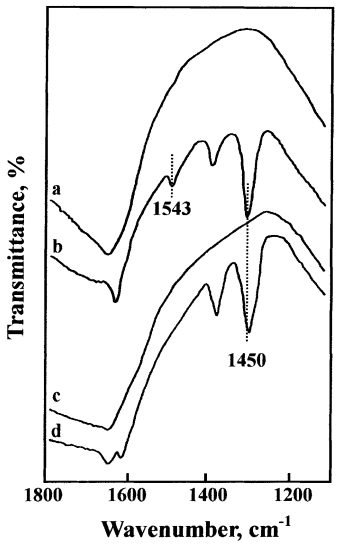

Fig. 12. IR spectra of pyridine adsorbed on catalyst A-7.4: (a) Background after evacuation at 100 °C for 2 h; (b) pyridine adsorbed on (a); (c) background after evacuation at 400 °C for 2 h; (d) pyridine adsorbed on (c); gas phase was evacuated at 200 °C for 1 h after adsorption in (b) and (d).

temperature, the catalytic activity solely depends on the temperature of the second evacuation [21]. For example, the catalyst evacuated at 500 °C was cooled in water vapor to room temperature and re-evacuated at 200 °C. The activity thus obtained was identical with that obtained by direct evacuation at 200 °C.

Applying this method, the mechanism of the activity decrease caused by the increase in evacuation temperature from 100 to 350 °C was elucidated with ethylene dimerization activity of catalyst A-7.4. The results are illustrated in Fig. 12, where black points indicate the catalytic activity of catalyst treated with water or oxygen. It is clear that the catalyst deactivated by evacuation at 350 or 600 °C can be reactivated by cooling in water vapor (200 Torr) followed by evacuation at 100 °C, while the cooling in oxygen (8 Torr) does not result in reactivation. An analogous result was obtained for the isomerization activity of catalyst A-10. The catalyst was first evacuated at 300 °C and cooled in water vapor. The second evacuation at 100 °C reproduced the peak activity.

It is accordingly concluded that the deactivation is caused by dehydration from the surface. The peak activity appears to be associated with an optimum content of water, suggesting that the acid sites responsible for the catalytic activity are protonic in nature. In fact, it has been shown by a tracer work that the butene isomerization on $NiO\text{-}SiO_2$ evacuated at 100 °C is catalyzed by the protonic acid [9]. The present results suggest that the protonic acid sites are also responsible for the ethylene dimerization. On the other hand the catalytic activities developed by evacuation at above 300 °C would be associated with non-protonic acid sites because those are developed by dehydration. The non-protonic nature of acid sites was previously shown with respect to the butene isomerization on $NiO\text{-}SiO_2$ evacuated at 500 °C [9].

4.6. Effect of acid strength on the catalytic activity of $NiO\text{-}TiO_2$ modified with acids

The catalytic activities for 1-butene isomerization were examined and the results are shown as a function of reaction time in Fig. 13. No product other than *cis*- and *trans*-2-butene was detected in the reaction mixture. When the NiO mol% of catalyst is 25 and the catalysts are evacuated at 400 °C for 1.5 h, the catalyst exhibited the highest activity. Therefore, in this paper emphasis is placed to the only catalyst

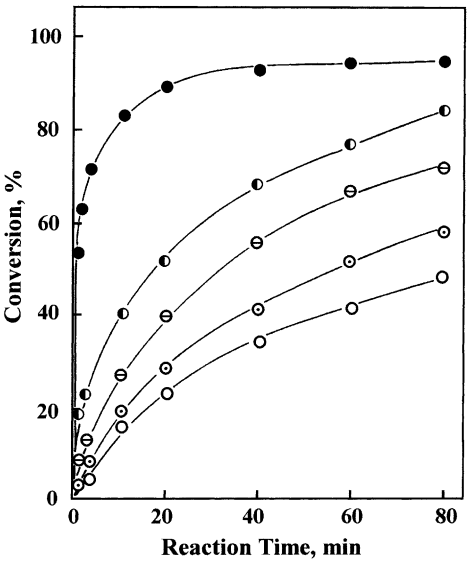

Fig. 13. Conversion of 1-butene against reaction time: (●) $NiO\text{-}TiO_2/SO_4^{2-}$; (◐) $NiO\text{-}TiO_2/PO_4^{3-}$; (⊖) $NiO\text{-}TiO_2/BO_3^{3-}$; (⊙) $NiO\text{-}TiO_2/SeO_4^{2-}$; (○) $NiO\text{-}TiO_2$.

having 25 mol% of NiO content and evacuated at 400 °C. After evacuation at 400 °C for 1.5 h, strong IR absorption bands of anions of acids were left to indicate a very strong interaction between anions and oxides and any decomposition or evaporation of anions were not observed. The content of anion in the catalysts after calcining at 400 °C was estimated to be about ~3–4 wt.%. As shown in Fig. 13, the catalysts modified with acids exhibited higher catalytic activity than the unmodified catalyst. NiO-TiO_2/SO_4^{2-} showed the most effective catalysis. Time course of isomerization was in agreement with the first rate law and the first-order rate constants are listed in Table 1. The order of catalytic activity was found to be NiO-TiO_2/SO_4^{2-} ≫ NiO-TiO_2/PO_4^{3-} > NiO-TiO_2/BO_3^{3-} > NiO-TiO_2/SeO_4^{2-} > NiO-TiO_2.

The catalytic activities for ethylene dimerization were also examined and the results are listed in Table 1, where the catalyst of 25 mol% of NiO was evacuated at 400 °C. NiO-TiO_2 alone without acid modification was totally inactive for the ethylene dimerization at room temperature unlike 1-butene isomerization. However, all the modified catalysts exhibited catalytic activity, showing the highest activity of NiO-TiO_2/SO_4^{2-} like the case of 1-butene isomerization. On all the NiO-TiO_2 modified with acids, the product obtained from the gas phase was exclusively *n*-butene, in analogy with nickel-containing catalysts [3,4,10,13,14]. However, a small amount of hexenes from the phase adsorbed on the catalyst surface was detected. The order of catalytic activity was the same as that for isomerization. These results indicate that the modification with acids enhances the catalytic activities for both 1-butene isomerization and ethylene dimerization and the 1-butene isomerization activity runs parallel with the ethylene dimerization activity.

It is interesting to examine how the activity of solid acid catalysts depends upon the acid strength. The acid strengths of the present samples modified with acids were examined by a color change method using a series of Hammett indicators [17,20] as described in the previous paper [10]. The catalysts were pre-treated in glass tubes by the same procedure as for the reactions. Since, it was very difficult to observe the color of indicators adsorbed on catalysts of high nickel oxide content, a low percentage of nickel oxide (4 mol%) was used in this experiment. The results are listed in Table 1, where '+' indicates that the color of the base form changed to that of the conjugate acid form. The acid strength of the sample without acid modification was found to be $Ho \leq -3.0$. However, the acid strength of NiO-TiO_2/SO_4^{2-}, NiO-TiO_2/PO_4^{3-}, NiO-TiO_2/BO_3^{3-} and NiO-TiO_2/SeO_4^{2-} were estimated to be $Ho \leq -14.5$, $Ho \leq -8.2$, $Ho \leq -5.6$ and $Ho \leq -5.6$, respectively. As described above, NiO-TiO_2 alone without acid modification, whose acid strength was found to be $Ho \leq -3.0$, was totally inactive for the dimerization of ethylene at room temperature, although it exhibited a low activity for the isomerization of 1-butene. These results indicate that ethylene dimerization requires acid sites stronger than $Ho \leq -3.0$ and that 1-butene isomerization takes place on relatively weak acid sites in comparison with ethylene dimerization. Clear dependence of catalytic

Table 1
Acid strength and catalytic activity of NiO-TiO_2 modified with acids

	pK_a value of indicator	NiO-TiO_2/SO_4^{2-}	NiO-TiO_2/PO_4^{3-}	NiO-TiO_2/BO_3^{3-}	NiO-TiO_2/SeO_4^{2-}	NiO-TiO_2
Hammett indicator						
Dicinnalacetone	−3.0	+	+	+	+	+
Benzalacetophenone	−5.6	+	+	+	+	−
Anthraquinone	−8.2	+	+	−	−	−
Nitrobenzene	−12.4	+	−	−	−	−
2,4-Dinitrofluorobenzene	−14.5	+	−	−	−	−
Catalytic activity for isomerization ($k \times 10^2\ s^{-1}\ g^{-1}$)		11.66	3.32	2.22	1.47	0.81
Catalytic activity for dimerization (mmol g^{-1} 5 min^{-1})		2.71	1.32	0.98	0.96	0
Surface area ($m^2\ g^{-1}$)		234.1	235.2	229.8	227.4	189.6

activity upon acid strength is shown in Table 1. However, the discrepancy between the catalytic activities of $NiO\text{-}TiO_2/BO_3^{3-}$ and $NiO\text{-}TiO_2/SeO_4^{2-}$ having the same acid strength is probably due to the fact that no indicators with pK_a between −5.6 and −8.2 were used. The high catalytic activities of modified catalysts were correlated with the increase of acid strength by the inductive effects which were different depending on the anions of acids treated for the modification.

4.7. Ethylene dimerization activity of $NiSO_4/\gamma\text{-}Al_2O_3$ and active sites

The catalytic activities of $NiSO_4/\gamma\text{-}Al_2O_3$ for the reaction of ethylene dimerization were examined and the results are shown as a function of $NiSO_4$ content in the Fig. 14, where the catalysts were evacuated at 600 °C for 1.5 h before reaction. It is confirmed that the catalytic activity gives a maximum at 20 wt.% of $NiSO_4$. This seems not to be correlated to the specific surface area, but closely correlated to the acidity of catalysts. The acidity of $NiSO_4/\gamma\text{-}Al_2O_3$ calcined at 600 °C was determined by the amount of NH_3 irreversibly adsorbed at 230 °C [17,20]. Here, the acidity is the sum of Lewis and Brönsted acidity. As listed in Table 2, the BET surface area attained a maximum when the $NiSO_4$ content in the catalyst is 5 wt.% and then showed gradually decrease with increasing $NiSO_4$ content. However, as shown in Fig. 14, the more the acidity, the higher the catalytic activity. In this way it is demonstrated that the catalytic activity of $NiSO_4/\gamma\text{-}Al_2O_3$ substantially runs parallel to the total acidity, regardless of the nature of acidic site. In fact, it is known that either Lewis or Brönsted acidity is required for the ethylene dimerization [3].

The effect of evacuation temperature on the catalytic activity of $20\text{-}NiSO_4/\gamma\text{-}Al_2O_3$ was also examined,

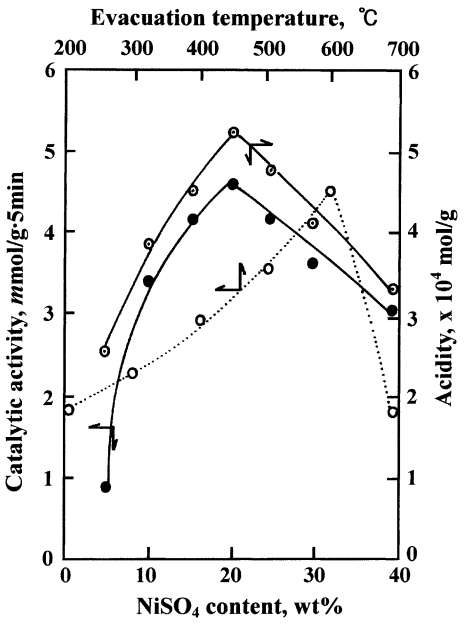

Fig. 14. Relationship between acidity and catalytic activity of $NiSO_4/\gamma\text{-}Al_2O_3$ for ethylene dimerization: (●) catalytic activity of $NiSO_4/\gamma\text{-}Al_2O_3$ having different for $NiSO_4$ content and evacuated at 600 °C; (○) catalytic activity of $20\text{-}NiSO_4/\gamma\text{-}Al_2O_3$ evacuated at different temperature; (⊙) acidity of $NiSO_4/\gamma\text{-}Al_2O_3$ having different $NiSO_4$ content and evacuation at 600 °C.

where the catalysts were evacuated for 1.5 h. As shown in Fig. 14, the maximum activity is obtained with the catalyst evacuated at 600 °C. To examine the effect of evacuation temperature on surface area, BET surface area of $20\text{-}NiSO_4/\gamma\text{-}Al_2O_3$ at various evacuation temperature (300–700 °C) was measured. However, the particular change of surface area was not observed, giving about 190–193 $m^2\,g^{-1}$ regardless of evacuation temperature. Therefore, it seems likely that the variation of catalytic activity is not

Table 2
Specific surface area of $NiSO_4/\gamma\text{-}Al_2O_3$ catalysts calcined at 600 °C

Catalyst	Surface area ($m^2\,g^{-1}$)	Catalyst	Surface area ($m^2\,g^{-1}$)
$\gamma\text{-}Al_2O_3$	240	$20\text{-}NiSO_4/\gamma\text{-}Al_2O_3$	193
$2\text{-}NiSO_4/\gamma\text{-}Al_2O_3$	287	$25\text{-}NiSO_4/\gamma\text{-}Al_2O_3$	159
$5\text{-}NiSO_4/\gamma\text{-}Al_2O_3$	290	$30\text{-}NiSO_4/\gamma\text{-}Al_2O_3$	139
$7\text{-}NiSO_4/\gamma\text{-}Al_2O_3$	225	$40\text{-}NiSO_4/\gamma\text{-}Al_2O_3$	130
$10\text{-}NiSO_4/\gamma\text{-}Al_2O_3$	217	$100\text{-}NiSO_4/\gamma\text{-}Al_2O_3$	25
$15\text{-}NiSO_4/\gamma\text{-}Al_2O_3$	210		

related to the change of surface area but to the easy formation of active site depending on the evacuation temperature. On all the catalysts of $NiSO_4/\gamma$-Al_2O_3, ethylene was selectively dimerized to *n*-butenes. In the composition of *n*-butenes analyzed by gas chromatography, 1-butene was found to predominate exclusively at the initial reaction time as compared with *cis*- and *trans*-butene. However, it was shown that the amount of 1-butene decreases with the reaction time, while the amount of 2-butene increases. Therefore, it seems likely that the initially produced 1-butene is also isomerized to 2-butene during the reaction.

γ-Al_2O_3 alone without $NiSO_4$ was totally inactive for the dimerization reaction at room temperature. The catalyst calcined at 900 °C, which has no sulfate ion due to the complete decomposition was inactive for dimerization. Therefore, the active site responsible for dimerization is suggested to consist of a low-valent nickel and an acid, as observed in the NiO-containing catalysts [10–12,16]. In fact, it is known that the sulfated alumina is an acid [22,23]. The term 'low-valent nickel' originated from the fact that the NiO-SiO_2 catalyst was drastically poisoned by carbon monoxide, since a low-valent nickel is prone to chemisorb carbon monoxide [16]. In this work, all catalysts added with $NiSO_4$ were poisoned by 1 μmol g^{-1} of carbon monoxide for dimerization. It seems that the formation of low-valent nickel is caused by evacuation at high temperature.

The IR spectra of CO adsorbed on 20-$NiSO_4/\gamma$-Al_2O_3 were examined to clarify the formation of low-valent nickel. When the sample was exposed to CO (50 Torr) at room temperature, the adsorbed CO band appeared at 2200 cm^{-1}, as shown in Fig. 15. The band might be assigned to the stretching vibration for CO adsorbed on Ni^{2+} [24,25]. However, when the sample evacuated at 600 °C for 1 h was exposed to CO (100 Torr), the two bands at 2170 and 2122 cm^{-1}, in addition to the band at 2200 cm^{-1}, were observed (Fig. 15). The intensities of two bands increased simultaneously with increasing CO concentration, as shown in Fig. 15. Therefore, it seems likely that the two bands originate from one species ($Ni^{+}(CO)_2$). The bands at 2170 and 2122 cm^{-1} are assigned to a symmetrical and asymmetrical stretching vibrations of $Ni^{+}(CO)_2$, respectively [24,25].

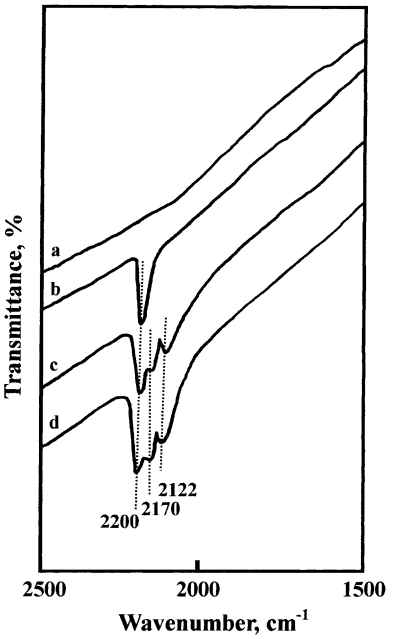

Fig. 15. IR spectra of CO adsorbed on 20-$NiSO_4/\gamma$-Al_2O_3: (a) background of 20-$NiSO_4/\gamma$-Al_2O_3 evacuated at room temperature; (b) after the introduction of 50 Torr CO to sample (a); (c) after introduction of 100 Torr CO to the sample evacuation at 600 °C for 1 h; (d) after the introduction of 150 Torr CO to the sample (c).

To obtain further information on the oxidation state of low-valent nickel species, Ni 2p XPS of 20-$NiSO_4/\gamma$-Al_2O_3 was measured and the results are shown in Fig. 16. For the sample evacuated at room temperature, the vertical lines at 856.9 eV (Ni $2p_{3/2}$) and 864.7 eV (Ni $2p_{1/2}$) in Fig. 16 indicate the positions of the peaks related to Ni^{2+}, in agreement with previous reports [26,27]. However, for the sample evacuated at 600 °C, the positions of the vertical lines were shifted to the lower binding energies, indicating the formation of low-valent nickel species by evacuation at 600 °C. In view of IR results and previous report [27], the vertical lines at 855.6 eV (Ni $2p_{3/2}$) and 862.3 eV (Ni $2p_{1/2}$) indicate the positions of the peaks related to low-valent nickel species, Ni^{+}. In view of IR and XPS results, it is concluded that the active sites responsible for ethylene dimerization consist of a low-valent nickel, Ni^{+} and an acid. It seems likely that a low-valent nickel, Ni^{+} plays the role of adsorption site for ethylene because all catalysts are poisoned by carbon monoxide for ethylene dimerization,

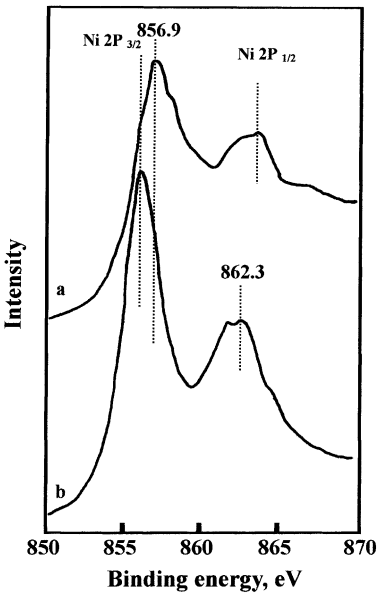

Fig. 16. The Ni 2p XPS of 20-$NiSO_4/\gamma$-Al_2O_3 calcined at 600 °C: (a) after evacuation at room temperature; (b) after evacuation at 600 °C for 1 h.

while acid sites are responsible for the formation of reaction intermediate, such as ethyl cation.

5. Conclusions

Nickel oxide-silica catalysts were prepared by precipitation from an acidic solution of a nickel salt–sodium silicate mixture. Two types of nickel-hydrosilicate, montmorillonite and antigorite were formed in the catalysts, the relative abundance of which was indicated by IR bands at 710 and 665 cm^{-1}. Catalytic activities of nickel silicates for ethylene dimerization and butene isomerization ran parallel when the catalysts were activated by evacuation at elevated temperatures, giving two maxima in activities. Variations in catalytic activities were closely correlated to the acidity of catalysts. The acid site responsible for the catalytic activity was protonic on montmorillonite, which non-protonic on antigorite, as evidenced by the effects of water content and the IR spectra of adsorbed pyridine.

Catalytic activities of $NiO\text{-}TiO_2$ catalysts modified with various acids for above two reactions depended upon the acid strength of catalysts. The order of catalytic activities for both reactions was found to be $NiO\text{-}TiO_2/SO_4^{2-} \gg NiO\text{-}TiO_2/PO_4^{3-} > NiO\text{-}TiO_2/BO_3^{3-} > NiO\text{-}TiO_2/SeO_4^{2-} > NiO\text{-}TiO_2$. In view of IR spectra of CO adsorbed on $NiSO_4/\gamma$-Al_2O_3 and XPS results, it is concluded that the active sites responsible for ethylene dimerization consist of a low-valent nickel (Ni^+) and an acid. It is suggested that a low-valent nickel (Ni^+) plays the role of adsorption site for ethylene, while acid sites are responsible for the formation of reaction intermediate, such as ethyl cation.

Acknowledgements

This work was supported by Grant no. 2001-1-30700-006-2 from the Basic Research Program of the Korea Science and Engineering Foundation. We wish to thank Korea Basic Science Institute (Taegu Branch) for the use of X-ray diffractometer.

References

[1] D. Kiessling, G. Wendt, K. Hagenau, R. Schöllner, Appl. Catal. 71 (1991) 69.
[2] J.R. Sohn, D.C. Shin, J. Catal. 160 (1996) 314.
[3] J.R. Sohn, A. Ozaki, J. Catal. 59 (1979) 303.
[4] G. Wendt, E. Fritsch, R. Schollner, H.Z. Siegel, Anorg. Allg. Chem. 467 (1980) 51.
[5] O.S. Morozova, G.N. Kryukova, A.V. Ziborov, L.M. Plyasova, J. Catal. 144 (1993) 50.
[6] G.F. Berndt, S.J. Thomson, G.J. Webb, Chem. Soc. Farad. Trans. 1 (79) (1983) 195.
[7] V.R. Choudhary, B.S. Uphade, A.S. Mamman, J. Catal. 172 (1997) 281.
[8] G. Wendt, D. Hentschel, J. Finster, R. Schöllner, J. Chem. Soc. Farad. Trans. 1 (79) (1983) 2013.
[9] A. Ozaki, K. Kimura, J. Catal. 3 (1964) 395.
[10] J.R. Sohn, H.J. Kim, J. Catal. 101 (1986) 428.
[11] J.R. Sohn, H.W. Kim, J.T. Kim, J. Mol. Catal. 41 (1989) 375.
[12] J.R. Sohn, H.W. Kim, M.Y. Park, E.H. Park, J.T. Kim, S.E. Park, Appl. Catal. 128 (1995) 127.
[13] L. Bonneviot, D. Olivier, M. Che, J. Mol. Catal. 21 (1983) 415.
[14] I.V. Elev, B.N. Shelimov, V.B. Kazansky, J. Catal. 89 (1984) 470.
[15] A.K. Ghosh, L.J. Kevan, J. Phys. Chem. 92 (1988) 4439.
[16] K. Kimura, H. A-I, A. Ozaki, J. Catal. 18 (1970) 271.
[17] J.R. Sohn, S.Y. Lee, Appl. Catal. A Gen. 164 (1997) 127.
[18] G.A. Martin, B. Imelik, M. Prettre, C.R. Acad. Sci. Paris 264 (1967) 1536.
[19] V. Stubican, R. Roy, Z. Kristallogr. 115 (1961) 200.

[20] J.R. Sohn, S.G. Cho, Y.I. Pae, S. Hayashi, J. Catal. 159 (1996) 170.
[21] T. Shiba, A. Ozaki, Nippon Kagaku Zasshi 74 (1953) 295.
[22] T. Jin, T. Yamaguchi, K. Tanabe, J. Phys. Chem. 90 (1986) 4794.
[23] O. Saur, M. Bensitel, A.B.M. Saad, J.C. Lavalley, C.P. Tripp, B.A. Morrow, J. Catal. 99 (1986) 104.
[24] M. Kemarec, D. Oliver, M. Richord, M. Che, F. Bozon-verduraz, J. Phys. Chem. 86 (1986) 2818.
[25] P.H. Kasai, R.J. Bishop Jr, J. Phys. Chem. 82 (1978) 279.
[26] F. van Looij, J.W. Geus, J. Catal. 168 (1997) 154.
[27] J.C. de Jesus, P. Pereira, J. Carrazza, F. Zaera, Surf. Sci. 369 (1996) 217.